

Coexistence of bond-order wave and antiferromagnetism in a two-dimensional half-filled Peierls-Hubbard model

Qingshan Yuan^{1,2} and Thilo Kopp¹

¹ *Experimentalphysik VI, Universität Augsburg, 86135 Augsburg, Germany*

² *Pohl Institute of Solid State Physics, Tongji University, Shanghai 200092, P.R.China*

Abstract

The two-dimensional Peierls-Hubbard model is studied at half-filling within both Hartree-Fock and Kotliar-Ruckenstein slave-boson theory. The interplay between two types of long-range order, bond-order wave (BOW) and antiferromagnetism (AFM), is analysed for two representative dimerization patterns, corresponding both to the same wavevector (π, π) . For each pattern, the Peierls dimerization (and associated BOW) is weakened and finally suppressed with increasing Hubbard on-site interaction, and correspondingly AFM is gradually enhanced. In particular, a coexistence regime with both BOW and AFM order is established in the parameter space of electron-lattice and Hubbard interactions.

PACS numbers: 71.45.Lr, 71.10.Fd, 75.30.Fr, 63.20.Kr

I. INTRODUCTION

The Peierls instability towards spatially broken symmetry is an important phenomenon in low dimensional materials [1]. The one-dimensional (1D) case has been widely discussed in the context of polyacetylene $(\text{CH})_x$ based on the Su-Schrieffer-Heeger (SSH) model [2,3], where lattice displacements couple to electron hopping. For a half-filled band arbitrary small electron-lattice (e-l) coupling will induce a lattice dimerization (disregarding quantum lattice fluctuations), which is associated with a periodic modulation of the bond hopping, that is, a so called on-bond charge-density wave or bond-order wave (BOW) [4]. It has been established that the Hubbard on-site Coulomb electron-electron (e-e) interaction U will enhance the bond alternation initially for small values and finally suppress it at large values of U [5–7].

In two dimensions few theoretical investigations exist [7–11], some of which connect the physics of Peierls systems to that of the high- T_c copper oxides [8,9]. Moreover, these investigations may be of direct relevance to those quasi-two dimensional (2D) materials which show a Peierls instability such as transition-metal oxide bronzes like $\text{AMo}_6\text{O}_{17}$ ($\text{A}=\text{Na}, \text{K}, \text{Tl}$) [12] and organic conductors like $(\text{BEDT-TTF})_2\text{MHg}(\text{SCN})_4$ ($M=\text{K}, \text{Rb}, \text{Tl}$) [13,10]. As an effective minimal model, in this context, the 2D version of the SSH model was investigated [8,9,11]. With only nearest-neighbour (n.n.) hopping on a square lattice, the electronic Fermi surface is perfectly nested at half-filling with nesting vector $Q = (\pi, \pi)$. Two possible alternation patterns for the lattice distortion and the concurrent bond hopping comply with this Q , as illustrated in Fig. 1. Whereas for pattern (a) the dimerization is in both directions, it is only in one direction for pattern (b) [8]. Similar to the 1D case, already for an infinitesimal e-l coupling, the 2D SSH model goes through a Peierls instability into one of the dimerized states of Fig. 1 [11].

When a Hubbard on-site Coulomb interaction U is included — the model is then the so called Peierls-Hubbard model, results differ from the 1D case. Numerical calculations on a small 2D lattice [8,9] indicated that the Peierls instability will be suppressed by the

Hubbard U [14]. An intuitive explanation is that the on-site Coulomb interaction favors a spin-density wave (SDW) long-range order, that is, antiferromagnetism (AFM), while the dimerization associated with BOW harmonizes with a spin-singlet formation between those two n.n. spins which are connected by a strong bond. As we know, due to the same nesting effect, the pure 2D half-filled Hubbard model (without consideration of a Peierls instability) has been shown to exhibit AFM long-range order for any $U > 0$. This is in stark contrast to the corresponding 1D case where no true long-range AFM order is available and the correlated state rather corresponds to a resonant valence bond state with strong weight from n.n. singlets [15]. Consequently, one may envisage, for finite e-l coupling (denoted as η , see below) and e-e on-site interaction U , a competition between BOW and AFM as the underlying physics in the 2D half-filled Peierls-Hubbard model. In the large U limit, Zhang and Prelovsek have studied the corresponding spin-Peierls (SP) instability and found that the SP state, competing with AFM, does not appear unless the spin-lattice coupling (analogous to η here) exceeds a threshold [16].

The details of the competition between the two ordered states were studied only for the above limiting case and the situation is not clear for general values of η and U . In particular, a basic problem has to be solved: does BOW disappear once the AFM order sets in, or is a coexistence of the two orders possible? It was previously argued by Mazumdar within a real space approach that the appearance of the AFM should coincide with the disappearance of the BOW [9], which was, however, not verified. To clarify this issue — which is the topic of this paper, one needs to explicitly calculate the two order parameters for the BOW and AFM with varying η and/or U .

FIGURES

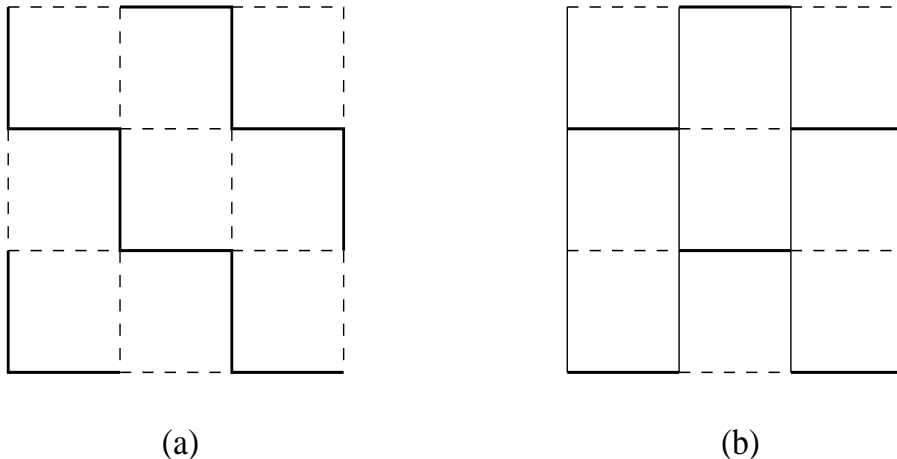


FIG. 1. The lattice distortion patterns (a) and (b). In the figure a thick solid line corresponds to a strong bond with hopping integral $t(1 + \delta)$, a dashed line corresponds to a weak bond with hopping integral $t(1 - \delta)$, and a thin solid line corresponds to a normal bond with hopping integral t . Both patterns correspond to phonons with wave vector (π, π) . The dimerization is along two axes for pattern (a), while only along the x axis for pattern (b).

In this paper we make use of both the Hartree-Fock (HF) and Kotliar-Ruckenstein slave-boson (SB) approach [17] to treat the Hubbard interaction. The HF results are usually valid at weak-coupling, and they can be used as a basis for further elaborate studies. In the context of investigations on density wave instabilities, the HF theory may give reasonable results even in one dimension [18], where one would expect it to be worst because of strong fluctuations. In dimensions higher than one, as considered here, qualitatively correct results are expected from the HF theory. In order to extend the controlled weak-coupling results to intermediate values of U , we evaluate BOW and AFM within a slave boson mean-field approach, which is considered to be appropriate to interpolate from weak to strong coupling [19].

The paper is organized as follows. In the next section the model Hamiltonian is introduced, and then the HF and SB approaches are formulated. The self-consistent equations for the order parameters are derived in both theories. In Sec. III numerical results are presented. The main results are shown in Fig. 2, where the coexistence of BOW and AFM

is found to be possible for each of the two patterns, in contrast to Mazumdar's argument. A complete comparison is made between the results derived from both approaches. Conclusive remarks are given in Sec. IV. An appendix completes the SB formulation.

II. FORMULATION

We begin with the 2D half-filled Peierls-Hubbard model

$$H = H_t + H_U + H_K \quad (1)$$

with

$$\begin{aligned} H_t &= -t \sum_{i,j,\sigma} [1 + \alpha(u_{i,j}^x - u_{i+1,j}^x)] (c_{i,j,\sigma}^\dagger c_{i+1,j,\sigma} + \text{h.c.}) \\ &\quad -t \sum_{i,j,\sigma} [1 + \alpha(u_{i,j}^y - u_{i,j+1}^y)] (c_{i,j,\sigma}^\dagger c_{i,j+1,\sigma} + \text{h.c.}) , \\ H_U &= U \sum_{i,j} n_{i,j,\uparrow} n_{i,j,\downarrow} , \\ H_K &= \frac{K}{2} \sum_{i,j} [(u_{i,j}^x - u_{i+1,j}^x)^2 + (u_{i,j}^y - u_{i,j+1}^y)^2] , \end{aligned}$$

where $c_{i,j,\sigma}^\dagger$ ($c_{i,j,\sigma}$) is the creation (annihilation) operator for an electron at site (i, j) with spin σ (i denotes x coordinate and j denotes y coordinate), $n_{i,j,\sigma}$ is defined as $n_{i,j,\sigma} = c_{i,j,\sigma}^\dagger c_{i,j,\sigma}$, $u_{i,j}^{x/y}$ is the displacement component of site (i, j) in x/y direction, t is the n.n. hopping parameter, and α is the electron-lattice coupling constant. H_U is the Hubbard on-site interaction with the repulsion strength U . The last term H_K is the lattice elastic potential energy, with K the elastic constant. The phonons are treated in adiabatic approximation.

For an analytical treatment on an infinite lattice, we have to work with a definite distorted lattice, rather than allowing the distortions to arise arbitrarily. In this paper we constrain the discussion to the lattice distortions within the two commonly used dimerization patterns shown in Fig. 1. Only these patterns correspond to the nesting vector $Q = (\pi, \pi)$ and they realize an unconditional Peierls instability that occurs for $\alpha \rightarrow 0$ and $U = 0$. Explicitly they are written as

$$u_{i,j}^x - u_{i+1,j}^x = (-1)^{i+j} u, \quad u_{i,j}^y - u_{i,j+1}^y = (-1)^{i+j} u$$

for pattern (a) and

$$u_{i,j}^x - u_{i+1,j}^x = (-1)^{i+j}u, \quad u_{i,j}^y - u_{i,j+1}^y = 0$$

for pattern (b). For convenience, two dimensionless parameters are defined: the dimerization amplitude $\delta = \alpha u$ and the electron-lattice coupling constant $\eta = \alpha^2 t / K$. Throughout the paper the hopping integral t is taken as the energy unit.

In the following we will construct the analytical formulas based on the HF and SB approaches, respectively, and leave the numerical calculations to the next section.

A. Hartree-Fock theory

In our model, the on-site charge density wave is not favored and the total electron number on each site is uniform and equal to one at half-filling. Then the expectation value of the electron density with a given spin may be simply assumed as $\langle n_{i,j,\sigma} \rangle = \frac{1}{2}[1 + \sigma(-1)^{i+j}m]$ when the AFM order is taken into account, where m represents the staggered magnetization. In HF approximation (equivalent to Hartree here) the local Hubbard term may be decoupled as $U \sum_{i,j} n_{i,j,\uparrow} n_{i,j,\downarrow} \rightarrow U \sum_{i,j} (n_{i,j,\uparrow} \langle n_{i,j,\downarrow} \rangle + \langle n_{i,j,\uparrow} \rangle n_{i,j,\downarrow} - \langle n_{i,j,\uparrow} \rangle \langle n_{i,j,\downarrow} \rangle)$. Then the Hamiltonian becomes quadratic and may be easily diagonalized in momentum space. Under consideration of a bipartite lattice the final electronic spectra are derived as follows for pattern (a) and (b), respectively,

$$\varepsilon_{\mathbf{k},a}^{\pm} = \pm \sqrt{U^2 m^2 / 4 + 4[(\cos k_x + \cos k_y)^2 + \delta^2 (\sin k_x + \sin k_y)^2]}, \quad (2)$$

$$\varepsilon_{\mathbf{k},b}^{\pm} = \pm \sqrt{U^2 m^2 / 4 + 4[(\cos k_x + \cos k_y)^2 + \delta^2 \sin^2 k_x]}. \quad (3)$$

Each branch above ($-$ or $+$) is two-fold (spin) degenerate. The wave vector $\mathbf{k} = (k_x, k_y)$ is restricted to the reduced Brillouin zone: $-\pi < k_x \pm k_y \leq \pi$. With inclusion of constant terms the ground state energy is

$$E_{\nu} = 2 \sum_{\mathbf{k}} \varepsilon_{\mathbf{k},\nu}^{-} + NU(1 + m^2)/4 + E_{L,\nu},$$

where $\nu = a, b$ represent pattern (a) and (b), respectively, N is the total number of lattice sites and $E_{L,\nu}$ denote the lattice elastic energies for both patterns: $E_{L,a} = 2E_{L,b} = N\delta^2/\eta$.

The self-consistent equations for dimerization δ and magnetization m are found by minimization of the ground state energy. They read: $\partial E_\nu/\partial\delta = 0$ and $\partial E_\nu/\partial m = 0$. The latter results in (except for a trivial solution $m = 0$):

$$1 = \frac{U}{N} \sum_{\mathbf{k}} \frac{1}{|\varepsilon_{\mathbf{k},\nu}^-|}, \quad (4)$$

and the former leads to

$$1 = \frac{4\eta}{N} \sum_{\mathbf{k}} \frac{(\sin k_x + \sin k_y)^2}{|\varepsilon_{\mathbf{k},a}^-|} \quad (5)$$

for pattern (a) and

$$1 = \frac{8\eta}{N} \sum_{\mathbf{k}} \frac{\sin^2 k_x}{|\varepsilon_{\mathbf{k},b}^-|} \quad (6)$$

for pattern (b).

B. Slave-Boson theory

In the spirit of the Kotliar-Ruckenstein SB approach [17], four auxiliary bosons $e_{i,j}^{(\dagger)}$, $p_{i,j,\sigma}^{(\dagger)}$ ($\sigma = \uparrow, \downarrow$), $d_{i,j}^{(\dagger)}$ are introduced to label the four different states for an arbitrary site (i, j) , which can be empty, singly occupied by an electron with spin up or down, or doubly occupied. The unphysical states in the enlarged Hilbert space are eliminated by imposing two sets of local constraints:

$$e_{i,j}^\dagger e_{i,j} + \sum_{\sigma} p_{i,j,\sigma}^\dagger p_{i,j,\sigma} + d_{i,j}^\dagger d_{i,j} = 1 \text{ (completeness)}, \quad (7)$$

and

$$p_{i,j,\sigma}^\dagger p_{i,j,\sigma} + d_{i,j}^\dagger d_{i,j} = c_{i,j,\sigma}^\dagger c_{i,j,\sigma} \text{ (correctness of fermion occupancy for a given spin)}. \quad (8)$$

For a bipartite lattice, we introduce a set of bosons, with separate Lagrange multipliers for each sublattice. At the mean-field level, the bosons are replaced by c-numbers and assumed

to be site-independent on each sublattice. At the same time, the constraints above are softened to be satisfied only on the average on each sublattice. This treatment is equivalent to making a saddle-point approximation in the path-integral formulation. For concreteness, we introduce the following parametrization for sublattice A (and similar parameters are defined for sublattice B): e_A , $p_{A\sigma}$, d_A as average values of the boson operators $e_{i,j}^{(\dagger)}$, $p_{i,j,\sigma}^{(\dagger)}$, $d_{i,j}^{(\dagger)}$, respectively, and λ_A , λ_A^σ as Lagrange multipliers associated with the constraints (7), (8), respectively. Then the Hamiltonian (1) may be recast into the following form [we choose pattern (a) as an example]:

$$\begin{aligned}
H = & -t(1 + \delta) \sum_{R_{i,j} \in A, \sigma} z_\sigma (a_{i,j,\sigma}^\dagger b_{i+1,j,\sigma} + a_{i,j,\sigma}^\dagger b_{i,j+1,\sigma} + \text{h.c.}) \\
& -t(1 - \delta) \sum_{R_{i,j} \in B, \sigma} z_\sigma (b_{i,j,\sigma}^\dagger a_{i+1,j,\sigma} + b_{i,j,\sigma}^\dagger a_{i,j+1,\sigma} + \text{h.c.}) + NU(d_A^2 + d_B^2)/2 + E_{L,a} \\
& -\lambda_A \sum_{R_{i,j} \in A} (e_A^2 + \sum_\sigma p_{A\sigma}^2 + d_A^2 - 1) - \sum_{R_{i,j} \in A, \sigma} \lambda_A^\sigma (p_{A\sigma}^2 + d_A^2 - a_{i,j,\sigma}^\dagger a_{i,j,\sigma}) \\
& -\lambda_B \sum_{R_{i,j} \in B} (e_B^2 + \sum_\sigma p_{B\sigma}^2 + d_B^2 - 1) - \sum_{R_{i,j} \in B, \sigma} \lambda_B^\sigma (p_{B\sigma}^2 + d_B^2 - b_{i,j,\sigma}^\dagger b_{i,j,\sigma}), \quad (9)
\end{aligned}$$

where $a^\dagger(a)$ and $b^\dagger(b)$ are the electron creation (annihilation) operators for sublattice A and B, respectively. The hopping renormalization factor z_σ ensures the correct result in the limit of vanishing U and takes the form $z_\sigma = \langle z_\sigma^A \rangle \langle z_\sigma^B \rangle$ with

$$\langle z_\sigma^L \rangle = \frac{e_L p_{L\sigma} + p_{L\bar{\sigma}} d_L}{\sqrt{(1 - e_L^2 - p_{L\bar{\sigma}}^2)(1 - d_L^2 - p_{L\sigma}^2)}} \quad L = A, B.$$

The Hamiltonian (9) may be diagonalized in momentum space and the energy bands read:

$$\epsilon_{\mathbf{k}\sigma,a}^\pm = (\lambda_A^\sigma + \lambda_B^\sigma)/2 \pm \sqrt{(\lambda_A^\sigma - \lambda_B^\sigma)^2/4 + 4z_\sigma^2[(\cos k_x + \cos k_y)^2 + \delta^2(\sin k_x + \sin k_y)^2]}. \quad (10)$$

Similarly, the energy bands for pattern (b) are given by:

$$\epsilon_{\mathbf{k}\sigma,b}^\pm = (\lambda_A^\sigma + \lambda_B^\sigma)/2 \pm \sqrt{(\lambda_A^\sigma - \lambda_B^\sigma)^2/4 + 4z_\sigma^2[(\cos k_x + \cos k_y)^2 + \delta^2 \sin^2 k_x]}. \quad (11)$$

At half-filling and zero temperature only the two lower (−) bands are occupied (the constant $\lambda_A^\sigma + \lambda_B^\sigma$ is independent of σ as will be seen later). Then the ground state energy is expressed as ($\nu = a, b$)

$$E_\nu = \sum_{\mathbf{k}\sigma} \epsilon_{\mathbf{k}\sigma,\nu}^- + E_0 + E_{L,\nu} \quad (12)$$

with the constant $E_0 = (N/2)[U(d_A^2 + d_B^2) - \lambda_A(e_A^2 + \sum_\sigma p_{A\sigma}^2 + d_A^2 - 1) - \lambda_B(e_B^2 + \sum_\sigma p_{B\sigma}^2 + d_B^2 - 1) - \sum_\sigma \lambda_A^\sigma(p_{A\sigma}^2 + d_A^2) - \sum_\sigma \lambda_B^\sigma(p_{B\sigma}^2 + d_B^2)]$.

The self-consistent equations are obtained from the requirement that the ground state energy is stationary with respect to the parameters: $e_{A(B)}$, $p_{A(B)\sigma}$, $d_{A(B)}$, $\lambda_{A(B)}$, $\lambda_{A(B)}^\sigma$, δ . Except for the equation corresponding to δ , they all have the general form: $\sum_{\mathbf{k}\sigma} \partial \epsilon_{\mathbf{k}\sigma,\nu}^- / \partial X + \partial E_0 / \partial X = 0$, where X represents one of the parameters. Analyzing these equations and applying the constraint $\sum_\sigma p_{A(B)\sigma}^2 + 2d_{A(B)}^2 = \sum_\sigma \langle a(b)_{i,j,\sigma}^\dagger a(b)_{i,j,\sigma} \rangle = 1$ at half-filling, one may find the solution satisfying the following relations: $e_A = e_B = d_A = d_B (= d)$, $\lambda_A = \lambda_B (= \lambda)$, $p_{A\sigma} = p_{B\bar{\sigma}}$, $\lambda_A^\sigma = \lambda_B^{\bar{\sigma}}$ and $\sum_\sigma \lambda_A^\sigma = \sum_\sigma \lambda_B^\sigma = U$. Consequently, the number of free parameters is substantially reduced. The final compact self-consistent equations are listed in the Appendix with several re-defined independent parameters: d , λ , $\lambda_{AB} = \lambda_A^\uparrow - \lambda_B^\uparrow = \lambda_B^\downarrow - \lambda_A^\downarrow$, $m = p_{A\uparrow}^2 - p_{A\downarrow}^2 = p_{B\downarrow}^2 - p_{B\uparrow}^2$, where m denotes the same staggered magnetization as in HF theory.

III. NUMERICAL RESULTS AND DISCUSSIONS

We now focus on the numerical results obtained from the self-consistent equations. First, it is necessary to analytically analyze the mean-field equations more thoroughly. After a replacement of the momentum summation by integration, i.e., $\sum_{\mathbf{k}} \rightarrow \frac{N}{2\pi^2} \int \int_{-\pi/2}^{\pi/2} dk_1 dk_2$ ($k_{x,y} = \pm k_1 + k_2$), we examine Eq. (4) in HF theory. It is easily seen that the right-hand side (rhs) of Eq. (4) assumes a different analytical behavior for each of the two patterns due to their different respective spectra. For pattern (a) the rhs is divergent at $m = 0$, irrespective of the value of δ , and decreases monotonically with increasing m until it reaches a value less than 1 at $m = 1$. This implies for pattern (a) that Eq. (4) can be always solved with a nonzero solution of m as long as $U > 0$. For pattern (b) it is not always the case because the rhs is finite at $m = 0$ for any $\delta > 0$. Once this finite value is less than 1, one has to adopt the trivial $m = 0$ solution. The same conclusion may be obtained by a similar analysis of

the corresponding equations in the SB evaluation [see Eqs. (A3) and (A4) in the Appendix].

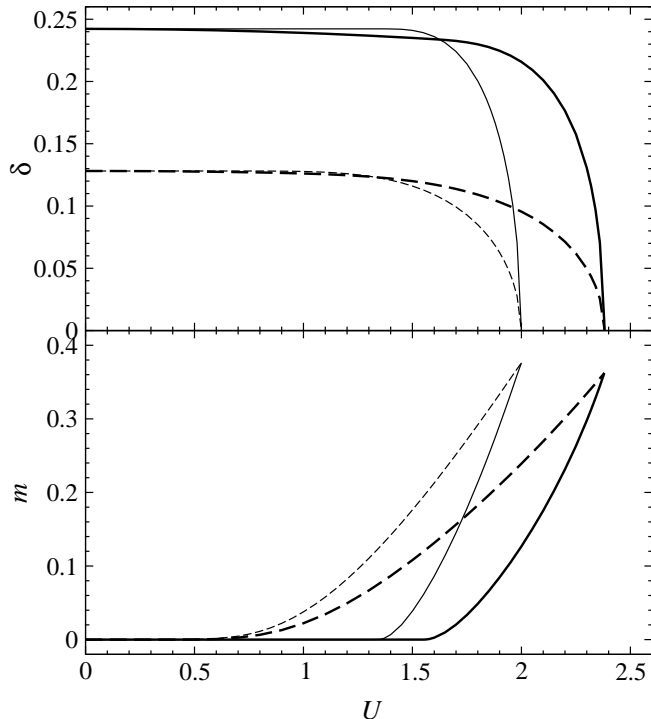


FIG. 2. The optimal values for the dimerization δ and AFM m as functions of U at $\eta = 0.5$. In each panel, the dashed lines are for pattern (a) and the solid ones are for pattern (b); the thick lines are the SB results and the thin ones are the HF results.

The numerical solutions for δ and m are displayed as functions of U in Fig. 2 for both patterns and in both approaches, whereby the e-l coupling η is fixed at 0.5. Globally, it is seen that for both patterns δ tends to decrease and m to increase with growing U . This supports the notion that the on-site interaction tends to favor the AFM order and to suppress the Peierls dimerization. Let us go to the details in the following.

In HF (see all the thin lines), it is found that for pattern (a) m becomes finite (although small at small U) and simultaneously δ begins to decrease once $U > 0$; while for pattern (b) m stays zero for small U up to $U > U_m \simeq 1.34$ where it becomes finite and correspondingly, δ first keeps its $U = 0$ value and then starts to decrease for $U > U_m$. The dimerization disappears at the same critical value $U_c \simeq 2$ for both patterns and it approaches zero smoothly and quickly when U is close to U_c . Comparing the results for m vs. U between the

two patterns, it is clear that pattern (a) is more favorable to the formation of AFM order than pattern (b). We will come to this point later.

Most of the above qualitative results are also found in SB approach (see all the thick lines). On the other hand, the difference to the HF results is clear as well, which we want to emphasize here. A distinct quantitative difference is that for each of the patterns the AFM order derived from SB theory is (much) weaker than that from HF theory, and correspondingly the dimerization decreases to zero over a larger range of U . The critical value for the disappearance of δ now becomes $U_c \simeq 2.38$, and the necessary Hubbard interaction to induce finite m in the case of pattern (b) is $U_m \simeq 1.56$. Both values are larger than the corresponding ones from the HF theory, which is understandable. As is well known, the HF theory usually overestimates the tendency towards AFM order. The SB theory, as an improved approach to fluctuation contributions, should lead to a slower formation of AFM, which complies with our findings.

A further important difference between the SB and HF results is observed in the region $U < U_m$ for pattern (b), where the AFM order has not yet formed. From the solid lines in the upper panel of Fig. 2, it is seen that the dimerization δ keeps a constant value in HF theory, while it decreases slowly with increase of U in SB theory. This disagreement may be understood as follows. In HF theory, see e.g., Eq. (3), the Hubbard U becomes irrelevant once the order parameter m is zero: the value for δ will be the same as that without U . In the SB approach, however, the Hubbard U is relevant even at $m = 0$ by affecting the probability of double occupancy d^2 . As U increases, the double occupancy is disfavored, i.e., the quantity d^2 decreases. Correspondingly the effective hopping tz_σ decreases too (cf. the expression for W in the Appendix), which may be understood equivalently as an increase of the elastic constant K or a reduction of the e-l coupling η . This signifies a decreasing dimerization. In this point the HF theory fails to catch the correct physics by assuming the probability of double occupancy as a constant $1/4$ which is correct only for $U \rightarrow 0$.

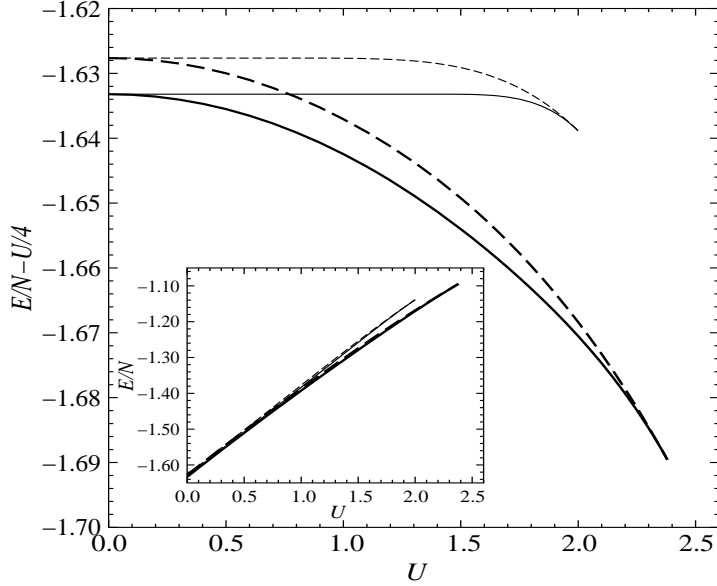


FIG. 3. The ground state energies (per site) as functions of U at $\eta = 0.5$, corresponding to Fig. 2 (with the same line labels). Each line stops at its own critical point U_c . The original values of these energies are shown in the inset. All energies are in units of t .

Furthermore, we can check the stability between both patterns by comparison of the ground state energies calculated in all cases, which are shown in Fig. 3. For each pattern the SB approach gives a lower energy than the HF theory in the whole range of U . Also, it is seen within each approach that pattern (b) has a lower energy than pattern (a), which signifies that pattern (b) is more stable.

It is worthwhile to point out that the BOW is always associated with the finite dimerization. In order to see this, we have calculated the BOW which is characterized by a modulation of the hopping amplitude. Explicitly, we define the expectation values $h_1^x = \langle a_{i,j,\sigma}^\dagger b_{i+1,j,\sigma} + \text{h.c.} \rangle$, $h_2^x = \langle b_{i,j,\sigma}^\dagger a_{i+1,j,\sigma} + \text{h.c.} \rangle$ (σ is irrelevant) for the alternating bond hoppings along the x axis, and similar values h_1^y, h_2^y for the hoppings along the y axis. By symmetry, we have $h_{1,2}^x = h_{1,2}^y$ for pattern (a) and $h_1^y = h_2^y$ for pattern (b). All the quantities are calculated in both theories and plotted as functions of U in Fig. 4. The BOW is exhibited by the inequality between h_1^x and h_2^x for each pattern [20]. It is clear for each approach that such an inequality is present within $0 < U < U_c$, the same region where the

dimerization is finite.

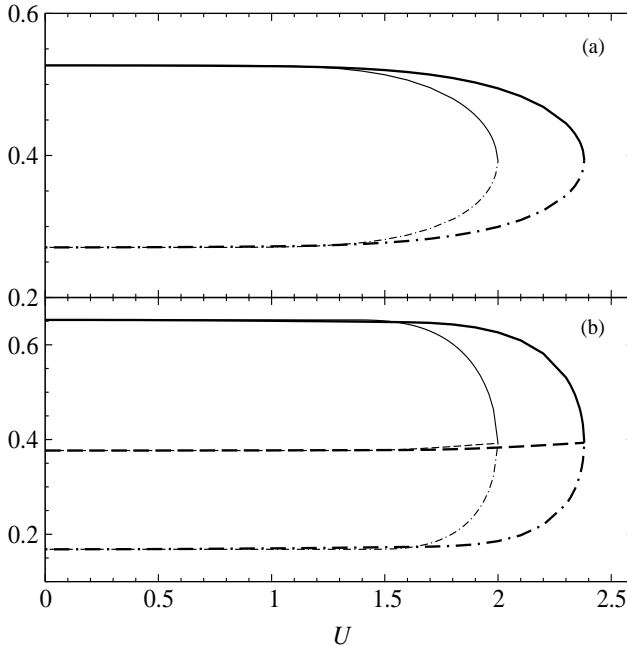


FIG. 4. The expectation values $h_{1,2}^x$, $h_{1,2}^y$ as functions of U for both patterns. In each panel, the solid lines show the quantity h_1^x and the dot-dashed lines give h_2^x ; the thick lines are the SB results and the thin ones are the HF results. For pattern (a), $h_{1,2}^y = h_{1,2}^x$. For pattern (b), $h_1^y = h_2^y$, which are plotted by the dashed lines in the lower panel.

Numerically, Tang and Hirsch [8] studied the same model and calculated the energy gain from dimerization as a function of U for the pattern (b) shown here. By studying how the energy gain changes with U , they found originally that the Hubbard U has little effect on the dimerization until it is large enough to suppress it, and later corrected that the dimerization is disfavored as soon as U is present. The finite-size effect was cautioned by the authors themselves. Their principal result, i.e., the Hubbard U is unfavorable to dimerization, is consistent with ours, especially with the SB results for pattern (b). Although it seems that the suppression of dimerization by U is faster in our results than what they displayed, no direct comparison is available because they calculated neither the order parameters nor the ground state energies. Obviously, further numerical calculations on large size systems are necessary for better comparison.

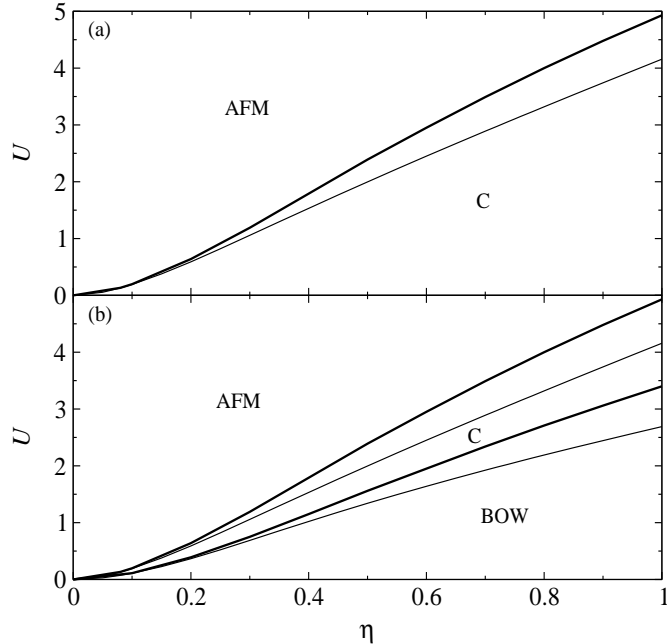


FIG. 5. Stable phases for BOW, AFM, and the coexisting state (C) in the parameter space (U, η) for pattern (a) [upper panel] and pattern (b) [lower panel]. The thick lines show the SB results and the thin ones show the HF results.

The main contribution in our work is that the order parameters as functions of U are explicitly obtained so that the interplay between BOW and AFM becomes transparent. The problem proposed in the Introduction is then naturally answered. It is clearly seen in Fig. 2 that the BOW and AFM may coexist for both patterns. For pattern (a) the coexistence (i.e., $\delta > 0$, $m > 0$) appears as long as $U > 0$ and pure AFM order exists for $U > U_c$. For pattern (b) the coexistence is limited to the region $U_m < U < U_c$. These results are not favorable to the argument by Mazumdar that the AFM emerges with the disappearance of the BOW [9]. In fact, the valence bond approach adopted by Mazumdar in real space is appealing. It states that, in order to implement a symmetry-broken state (e.g., BOW), “extreme configurations” with shortest repeat units have to be identified. For 2D systems, he chose pattern (a) as the realization of the Peierls state and argued that the extreme configuration for BOW is a combination of zigzag chains and the n.n. sites within each chain are doubly occupied and unoccupied, respectively. However, the pattern selected in

his work is not the pattern with the lowest energy and furthermore, the considered extreme configuration is actually disfavored, even for weak Coulomb on-site interaction, as is verified in the exact $U \rightarrow 0$ approach of this paper. It implies that spin fluctuations are more pronounced than charge fluctuations in the BOW state of the half-filled system.

Eventually, we determine the coexistence regions for different η in both theories. The results are shown in Fig. 5, where different phases are indicated in the parameter plane (U, η) . For pattern (a), only two phases exist, either a state with coexisting BOW and AFM or a pure AFM state. However for pattern (b) pure BOW and AFM states exist, which are separated by a coexisting state — the region between two thick (SB) or thin (HF) lines in Fig. 5. As for the methods, globally speaking, the SB approach pushes the AFM order to the higher U regime than the HF theory.

Finally, we come back to the difference between the results for the two patterns. As explained above, pattern (a) is more favorable to the development of AFM than pattern (b). It may be roughly understood from their different dimerization structures. As seen from Fig. 1, for pattern (b), each site is connected to only one n.n. site by a strong bond when the BOW (or dimerization) forms. Thus a spin singlet on this strong bond is apt to prevail in presence of U , which will resist the AFM. On the other hand, for pattern (a), each site connects two n.n. sites with strong bonds. This, on the contrary, makes the construction of spin singlets on these strong bonds difficult and the AFM is easier to develop.

IV. CONCLUSION

We have investigated the Peierls-Hubbard model in two dimensions at half-filling within both HF and SB approach. Two dimerization patterns, corresponding to the same wavevector (π, π) , are considered and the interplay between two long-range order states, BOW and AFM, is addressed. For each pattern, it is found that the Peierls dimerization (and associated BOW) is weakened by the on-site interaction U as soon as U is present and finally suppressed at a critical $U = U_c$. Correspondingly, the AFM is favored by U . Whereas for

pattern (a), see Fig. 2, AFM is induced once $U > 0$, it is not activated until $U = U_m$ for pattern (b). For both patterns, the coexistence of BOW and AFM is possible. SB and HF evaluations lead mostly to the same qualitative results and quantitatively the former approach results in larger values of U_c and U_m . Whereas the HF evaluation provides us with the exact weak coupling ($U \rightarrow 0$) result, the SB approach extends the findings to intermediate coupling, and corrects charge and spin fluctuation contributions beyond HF. Especially, the reduction of charge fluctuations by U decreases the dimerization δ consistently in the region $U < U_m$ for pattern (b).

ACKNOWLEDGEMENTS

We would like to thank T. Nunner for valuable discussions. This work was financially supported by the Deutsche Forschungsgemeinschaft through SFB 484. Q. Yuan also acknowledges S. Mazumdar, H. Zheng for useful communications and the support by the National Natural Science Foundation of China.

APPENDIX: SELF-CONSISTENT EQUATIONS IN THE SB THEORY

In this appendix we implement the formulation of the SB theory. With respect to the parameters d , λ , λ_{AB} , m , δ , the self-consistent equations are derived as follows for pattern (a):

$$d = -2C_1 I_2 / \lambda , \tag{A1}$$

$$-\lambda = U/2 + 2(C_2 / \sqrt{(1+m)/2 - d^2} + C_3 / \sqrt{(1-m)/2 - d^2}) I_2 , \tag{A2}$$

$$\lambda_{AB} = 4(C_3 / \sqrt{(1-m)/2 - d^2} - C_2 / \sqrt{(1+m)/2 - d^2}) I_2 , \tag{A3}$$

$$m = -\lambda_{AB} I_1 , \tag{A4}$$

$$1 = 4\eta W I_3 , \tag{A5}$$

where

$$\begin{aligned}
I_1 &= \frac{1}{N} \sum_{\mathbf{k}} \frac{1}{\sqrt{\lambda_{AB}^2/4 + 4W[(\cos k_x + \cos k_y)^2 + \delta^2(\sin k_x + \sin k_y)^2]}} , \\
I_2 &= \frac{1}{N} \sum_{\mathbf{k}} \frac{(\cos k_x + \cos k_y)^2 + \delta^2(\sin k_x + \sin k_y)^2}{\sqrt{\lambda_{AB}^2/4 + 4W[(\cos k_x + \cos k_y)^2 + \delta^2(\sin k_x + \sin k_y)^2]}} , \\
I_3 &= \frac{1}{N} \sum_{\mathbf{k}} \frac{(\sin k_x + \sin k_y)^2}{\sqrt{\lambda_{AB}^2/4 + 4W[(\cos k_x + \cos k_y)^2 + \delta^2(\sin k_x + \sin k_y)^2]}} , \\
W &= z_\sigma^2 = \frac{16d^4(\sqrt{(1+m)/2 - d^2} + \sqrt{(1-m)/2 - d^2})^4}{(1-m^2)^2} , \\
C_1 &= \frac{64d^3(\sqrt{(1+m)/2 - d^2} + \sqrt{(1-m)/2 - d^2})^3}{(1-m^2)^2} \times \\
&\quad \left\{ \frac{\sqrt{(1-m)/2 - d^2}[(1-m)/2 + d^2] + d^2\sqrt{(1+m)/2 - d^2}}{1-m} + m \rightarrow -m \right\} , \\
C_2 &= \frac{64d^4(\sqrt{(1+m)/2 - d^2} + \sqrt{(1-m)/2 - d^2})^3(1-d^2 + \sqrt{(1+m)/2 - d^2}\sqrt{(1-m)/2 - d^2})}{(1-m^2)^2(1-m)} , \\
C_3 &= \frac{64d^4(\sqrt{(1+m)/2 - d^2} + \sqrt{(1-m)/2 - d^2})^3(1-d^2 + \sqrt{(1+m)/2 - d^2}\sqrt{(1-m)/2 - d^2})}{(1-m^2)^2(1+m)} .
\end{aligned}$$

The equations for pattern (b) are the same as those above except that the expression $(\sin k_x + \sin k_y)^2$ in $I_{1,2,3}$ is substituted by $\sin^2 k_x$, and the Eq. (A5) is changed into

$$1 = 8\eta W I_3 . \quad (\text{A6})$$

Correspondingly, the ground state energies may be written in the simple form:

$$E_a = -2 \sum_{\mathbf{k}} \sqrt{\lambda_{AB}^2/4 + 4W[(\cos k_x + \cos k_y)^2 + \delta^2(\sin k_x + \sin k_y)^2]} + NUd^2 - Nm\lambda_{AB}/2 + E_{L,a}$$

for pattern (a) and

$$E_b = -2 \sum_{\mathbf{k}} \sqrt{\lambda_{AB}^2/4 + 4W[(\cos k_x + \cos k_y)^2 + \delta^2 \sin^2 k_x]} + NUd^2 - Nm\lambda_{AB}/2 + E_{L,b}$$

for pattern (b).

We point out that for both patterns there always exists a trivial solution with $m = 0$ [consider Eqs. (A3) and (A4) and note that $C_2 = C_3$ at $m = 0$]. Moreover, we checked that for $\delta = 0$ the results presented by Frésard *et al.* (e.g., staggered magnetization, ground state energy) for the pure Hubbard model [19] are reproduced.

REFERENCES

- [1] R. Peierls, *Quantum theory of solids* (Oxford University, Oxford, 1955).
- [2] A. J. Heeger, S. Kivelson, J. R. Schrieffer and W. P. Su, *Rev. Mod. Phys.* **60**, 781 (1988).
- [3] G. Grüner, *Density Waves in Solids* (Addison-Wesley, Redwood City, 1994).
- [4] For a Holstein-type (i.e., intrasite) electron-lattice coupling model, the lattice dimerization is associated with an on-site charge density wave.
- [5] S. Kivelson and D. E. Heim, *Phys. Rev. B* **26**, 4278 (1982).
- [6] S. Mazumdar and S. N. Dixit, *Phys. Rev. Lett.* **51**, 292 (1983); S. N. Dixit and S. Mazumdar, *Phys. Rev. B* **29**, 1824 (1984); J. E. Hirsch, *Phys. Rev. Lett.* **51**, 296 (1983).
- [7] J. A. Majewski and P. Vogl, *Phys. Rev. B* **46**, 12219 (1992).
- [8] S. Tang and J. E. Hirsch, *Phys. Rev. B* **37**, 9546 (1988); **39**, 12327 (1989).
- [9] S. Mazumdar, *Phys. Rev. B* **39**, 12324 (1989); **36**, 7190 (1987).
- [10] S. Mazumdar, S. Ramasesha, R. T. Clay, and D. K. Campbell, *Phys. Rev. Lett.* **82**, 1522 (1999); S. Mazumdar, R. T. Clay, and D. K. Campbell, *Phys. Rev. B* **62**, 13400 (2000).
- [11] Q. S. Yuan, T. Nunner and T. Kopp, *Eur. Phys. J. B* **22**, 37 (2001); Q. S. Yuan, preprint.
- [12] C. Schlenker, J. Dumas, M. Greenblatt and S. van Smaalen (Eds.), *Physics and Chemistry of Low-Dimensional Inorganic Conductors*, NATO ASI Series B: Physics Vol. 354 (Plenum, New York, 1996).
- [13] T. Sasaki and N. Toyota, *Synth. Metals* **70**, 849 (1995); K. Miyagawa, A. Kawamoto,

- and K. Kanoda, Phys. Rev. B **56**, R8487 (1997).
- [14] This conclusion is even true for arbitrary long-range interaction, see J. N. Liu, X. Sun, R. T. Fu, and K. Nasu, Phys. Rev. B **46**, 1710 (1992).
- [15] P. W. Anderson, Science **235**, 1196 (1987); L. Hulthén, Ark. Mat. Astron. Fys. **26A**, 1 (1938).
- [16] F. C. Zhang and P. Prelovsek, Phys. Rev. B **37**, 1569 (1988).
- [17] G. Kotliar and A. E. Ruckenstein, Phys. Rev. Lett. **57**, 1362 (1986).
- [18] For recent references, see, e.g., H. Fukuyama, H. Seo, and H. Kino, Physica B **280**, 462 (2000); S. Caprara, M. Avignon, and O. Navarro, Phys. Rev. B **61**, 15667 (2000); S. Gupta, S. Sil, and B. Bhattacharyya, Phys. Rev. B **63**, 125113 (2001).
- [19] R. Frésard, M. Dzierzawa, and P. Wölfle, Europhys. Lett. **15**, 325 (1991); R. Frésard and P. Wölfle, J. Phys.: Condens. Matter **4**, 3625 (1992).
- [20] Actually, if one defines a BOW order parameter $\frac{1}{N} \sum_{i,j} (-1)^{i+j} \langle c_{i,j,\sigma}^\dagger c_{i+1,j,\sigma} + \text{h.c.} \rangle$, it is equal to $(h_1^x - h_2^x)/2$.